
FedPara: Low-rank Hadamard Product Parameterization for Efficient Federated Learning

Nam Hyeon-Woo, Moon Ye-Bin, Tae-Hyun Oh
Department of Electrical Engineering
POSTECH
{hyeonw.nam, ybmoon, taehyun}@postech.ac.kr

Abstract

To overcome the burdens on frequent model uploads and downloads during federated learning (FL), we propose a communication-efficient re-parameterization, FedPara. Our method re-parameterizes the model's layers using low-rank matrices or tensors followed by the Hadamard product. Different from the conventional low-rank parameterization, our method is not limited to low-rank constraints. Thereby, our FedPara has a larger capacity than the low-rank one, even with the same number of parameters. It can achieve comparable performance to the original models while requiring 2.8 to 10.1 times lower communication costs than the original models, which is not achievable by the traditional low-rank parameterization. Moreover, the efficiency can be further improved by combining our method and other efficient FL techniques because our method is compatible with others. We also extend our method to a personalized FL application, pFedPara, which separates parameters into global and local ones. We show that pFedPara outperforms competing personalized FL methods with more than three times fewer parameters.

1 Introduction

Federated Learning (FL) [1] has been proposed as an efficient collaborative learning strategy along with the advance and spread of mobile and IoT devices. FL allows us to leverage locally stored private data and local computing resources of edge devices without directly accessing data by others, which improves communication efficiency while reducing privacy and security risks. FL is efficient in terms of reduced communication rounds. Although FL reduces total communication rounds for convergence by several local SGD epochs, the amount of transferred data at each round may not be acceptable to devices with bandwidth constraints or countries with low-quality communication infrastructure.¹ For instance, in typical image classification tasks, hundreds of millions of model parameters should be transferred through uplink and downlink at each training round for typical models [3, 4]. It also introduces an energy consumption challenge because wireless communication is significantly more power-intensive than computation [5, 6].

In this work, we propose a communication-efficient re-parameterization, FedPara, which reduces the number of bits transferred per round. To improve the communication efficiency of FL, the prior arts introduce new loss functions [7–9], delicate aggregation mechanisms [10, 11] at the server-side, and model quantization [12, 13] to compress uploading models. FedPara is an orthogonal approach to the above prior works because our FedPara does not change the optimization part but re-defines each layer's internal structure. FedPara directly re-parameterizes each fully-connected (FC) and convolutional layer of the model to have a small and factorized form while preserving the model's capacity and saving the bandwidth of uplink and downlink. Our key idea is to combine the

¹The gap between the fastest and the lowest communication speed across countries is significant; approximately 63 times different [2].

Hadamard product with low-rank parameterization as $\mathbf{W} = (\mathbf{X}_1 \mathbf{Y}_1^\top) \odot (\mathbf{X}_2 \mathbf{Y}_2^\top) \in \mathbb{R}^{m \times n}$, called *low-rank Hadamard product*. When $\text{rank}(\mathbf{X}_1 \mathbf{Y}_1^\top) = \text{rank}(\mathbf{X}_2 \mathbf{Y}_2^\top) = r$, then $\text{rank}(\mathbf{W}) \leq r^2$. This outstanding property facilitates spanning a full-rank matrix with much fewer parameters than the typical matrix of size $m \times n$. It significantly reduces the communication burdens during training. At the inference phase, we pre-compose and maintain \mathbf{W} that boils down to its original structure; thus, FedPara does not alter computational complexity at the inference time.

We demonstrate the effectiveness of FedPara on various classification benchmark datasets: CIFAR-10, CIFAR-100, and CINIC-10 for both IID and non-IID settings. The accuracy of our parameterization outperforms that of the low-rank parameterization baseline given the same number of parameters. Besides, FedPara has comparable accuracy to original counterpart models, and we observe that the accuracy is increased further as the number of parameters is increased. We also combine FedPara with other FL efficient algorithms to improve communication efficiency further.

We extend FedPara to the personalized FL application, named pFedPara, which separates the roles of each sub-matrix into global and local inner matrices. The global and local inner matrices learn the globally shared common knowledge and client-specific knowledge, respectively. We demonstrate performance improvement and robustness of pFedPara against competing algorithms on the subset of FEMNIST and MNIST. We devise three scenarios according to the amount and heterogeneity of local data for personalization experiments. We summarize our main contributions as follows:

- We propose the communication-efficient parameterization, FedPara, using the low-rank parameterization and the Hadamard product. We show that, unlike traditional low-rank parameterization, FedPara can span a full-rank matrix and tensor with reduced parameters. We also show that FedPara requires up to ten times fewer total communication costs than the original counterpart model to achieve target accuracy. FedPara even outperforms the original model by adjusting ranks.
- We show that our FedPara can be combined with other FL methods to get mutual benefits, which further increase accuracy and communication efficiency.
- We propose the personalizable FedPara, pFedPara, which splits the model into global and local parameters. The Hadamard product fuses these parameters to acquire a personalized model. pFedPara shows more robust results in challenging regimes than competing methods.

2 Related Work

Federated Learning. Federated optimization [14] minimizes the weighted sum of clients’ objective functions. FL typically consists of the following steps: (1) clients download the global shared model from the central server, (2) clients locally update each model using their own private data without accessing the others’ data, (3) clients upload their local models back to the server, and (4) the server consolidates the updated models and repeats these steps until the global model converges.

The most popular and de-facto algorithm, FedAvg [1], reduces communication costs by updating the global model using a simple model averaging once a large number of local SGD iterations per round. Thus, it improves the communication efficiency by a factor of the local SGD iterations per round compared to distributed learning. FedAvg shows powerful empirical performance with convergence guarantees under diverse settings [15–17].

Several variants [7–11, 18, 19] of FedAvg have been proposed to overcome the remaining challenges of data heterogeneity or convergence instability. They improve the communication efficiency by enhancing the convergence behavior of optimizers, whereby they reduce the number of necessary rounds until convergence. Unlike the above methods, our FedPara reduces communication costs directly by re-parameterizing learnable layers. Our approach can be combined with the aforementioned approaches to increase communication efficiency and convergence stability further.

Gradient Compression. In distributed learning, gradient compression approaches, including quantization [20–22, 12, 13] and sparsification [23, 24], have been developed to deal with communication traffic. signSGD [21] compresses gradients as 1-bit and aggregates gradient directions by voting. Lin *et al.* [24] employ the gradient sparsification algorithm, where local nodes send sparse gradients of which magnitudes exceed a threshold.

Gradient compression can be applied in FL by computing the difference between the global and local models as pseudo gradients. FedPAQ [12] and FedCOM [13] combine gradient quantization with

FedAvg and apply it to pseudo gradients to decrease upload costs. Our re-parameterization exploits the mathematical properties of matrix composition and is an orthogonal approach to the gradient manipulation ones; thus, our method can be integrated with gradient compression.

Model Decomposition. Model compression, such as quantization, pruning, and decomposition, facilitates model deployment on edge devices having limited memory and computational resources. Model decomposition is the mainstream of model compression strategies, which removes redundant and unnecessary filters. Decomposition methods are applied to matrices or tensors to approximate original layers with low-rank factorization. Lebedev *et al.* [25] use CP-decomposition and non-linear iterative optimization to replace an original fourth-order tensor with a low-rank tensor. Tai *et al.* [26] first reshape the tensor to a matrix form and apply low-rank decomposition by singular value decomposition (SVD). Phan *et al.* [27] increase the stability of low-rank tensor decomposition by considering sensitivity.

Most of these methods heavily depend on fine-tuning to compensate and recover the compatibility between layers lost by decomposition. Such a property is inappropriate for FL, where the model is collaboratively trained from scratch. Konečný *et al.* [28] train the model from scratch with low-rank constraints, but the accuracy is degraded when they set a high compression rate. Restricting the matrix space by low-rank constraints yields the limitation of model expressiveness. Compared to traditional low-rank parameterization, our factorized form can construct full-rank matrices and tensors. By virtue of our new parameterization, our method is not restricted by low-rank constraints despite the use of the low-rank parameterization. Moreover, it has no such limitation of expressiveness in theory. Empirically, the models re-parameterized by our method show comparable accuracy to the original counterparts when trained from scratch; thus, our FedPara is best suitable for FL.

3 Method

In this section, we first provide the overview of three popular low-rank parameterizations in Section 3.1 and present our proposed parameterization, FedPara, with its algorithmic properties in Section 3.2. Then, we extend FedPara to the personalized FL application, pFedPara, in Section 3.3.

Notations. We denote the Hadamard product as \odot , the Kronecker product as \otimes , n -mode tensor product as \times_n , and the i -th unfolding of the tensor $\mathcal{T}^{(i)} \in \mathbb{R}^{k_i \times \prod_{j \neq i} k_j}$ given a tensor $\mathcal{T} \in \mathbb{R}^{k_1 \times \dots \times k_n}$.

3.1 Overview of Low-rank Parameterization

The low-rank decomposition in neural networks has been typically applied to pre-trained models for compression [27], as post-decomposition, whereby the number of parameters is reduced while minimizing loss of encoded information. Given a learned parameter matrix $\mathbf{W} \in \mathbb{R}^{m \times n}$, it is formulated as finding the best rank- r approximation, as $\arg \min_{\widetilde{\mathbf{W}}} \|\mathbf{W} - \widetilde{\mathbf{W}}\|_F$ such that $\widetilde{\mathbf{W}} = \mathbf{X}\mathbf{Y}^\top$, where $\mathbf{X} \in \mathbb{R}^{m \times r}$, $\mathbf{Y} \in \mathbb{R}^{n \times r}$, and $r \ll \min(m, n)$. It reduces the number of parameters from $O(mn)$ to $O((m+n)r)$, and its closed-form optimal solution can be found by SVD.

This matrix decomposition is applicable to the FC layers and the reshaped kernels of the convolution layers. However, the natural shape of a convolution kernel is a fourth-order tensor; thus, the low-rank tensor decomposition, such as Tucker and CP decomposition, can be a more suitable approach [25, 27]. Given a learned high-order tensor $\mathcal{T} \in \mathbb{R}^{k_1 \times \dots \times k_n}$, Tucker decomposition multiplies a kernel tensor $\mathcal{K} \in \mathbb{R}^{r_1 \times \dots \times r_n}$ with matrices $\mathbf{X}_i \in \mathbb{R}^{r_i \times n_i}$, where $r_i = \text{rank}(\widetilde{\mathcal{T}}^{(i)})$ as $\widetilde{\mathcal{T}} = \mathcal{K} \times_1 \mathbf{X}_1 \times_2 \dots \times_n \mathbf{X}_n$, and CP decomposition is the summation of rank-1 tensors as $\widetilde{\mathcal{T}} = \sum_{i=1}^r \mathbf{x}_i^1 \times \mathbf{x}_i^2 \times \dots \times \mathbf{x}_i^n$, where $\mathbf{x}_i^j \in \mathbb{R}^{k_j}$. Likewise, it also reduces the number of model parameters.

In the FL context, where the parameters are continuously transferred between clients and the server during training, the reduced parameters lead to communication cost reduction, which is the main focus of this work. The post-decomposition approaches using SVD, Tucker, and CP decompositions do not improve the communication costs because those are applied to the original parameterization after finishing training. That is, the original large-size parameters are transferred during training in FL, and the number of parameters is reduced later after finishing training.

We take a different notion from the low-rank parameterizations. In the FL scenario, we train a model from scratch with low-rank constraints, but more specifically with *low-rank Hadamard product*

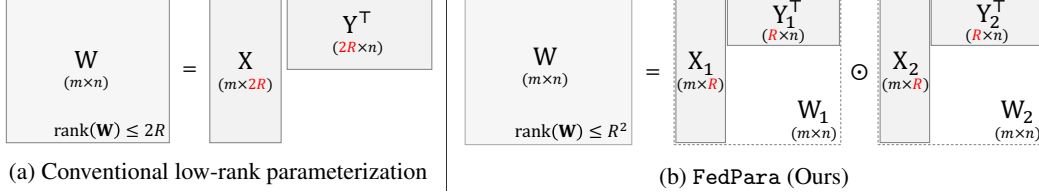


Figure 1: Illustrations of low-rank matrix parameterization and FedPara with the same number of parameters $2R(m+n)$. (a) Low-rank parameterization is the summation of $2R$ number of rank-1 matrices, $\mathbf{W} = \mathbf{X}\mathbf{Y}^\top$, and $\text{rank}(\mathbf{W}) \leq 2R$. (b) FedPara is the Hadamard product of two low-rank inner matrices, $\mathbf{W} = \mathbf{W}_1 \odot \mathbf{W}_2 = (\mathbf{X}_1\mathbf{Y}_1^\top) \odot (\mathbf{X}_2\mathbf{Y}_2^\top)$, and $\text{rank}(\mathbf{W}) \leq R^2$.

re-parameterization. We re-parameterize each learnable layer, including FC and convolutional layers, and train the surrogate model by FL. Different from Konečný et al. [28], our parameterization has comparable accuracy to the original counterpart model even when trained from scratch.

3.2 FedPara: A Communication-Efficient Parameterization

As aforementioned, the conventional low-rank parameterization has limited expressiveness due to its low-rank constraint. To overcome this while maintaining fewer parameters, we present our low-rank Hadamard product parameterization, called FedPara, which has the favorable property as follows:

Proposition 1 Let $\mathbf{X}_1 \in \mathbb{R}^{m \times r_1}$, $\mathbf{X}_2 \in \mathbb{R}^{m \times r_2}$, $\mathbf{Y}_1 \in \mathbb{R}^{n \times r_1}$, $\mathbf{Y}_2 \in \mathbb{R}^{n \times r_2}$, $r_1, r_2 \leq \min(m, n)$ and the constructed matrix be $\mathbf{W} := (\mathbf{X}_1\mathbf{Y}_1^\top) \odot (\mathbf{X}_2\mathbf{Y}_2^\top)$. Then, $\text{rank}(\mathbf{W}) \leq r_1r_2$.

Proof. $\mathbf{X}_1\mathbf{Y}_1^\top$ and $\mathbf{X}_2\mathbf{Y}_2^\top$ can be expressed as the summation of rank-1 matrices such that $\mathbf{X}_i\mathbf{Y}_i^\top = \sum_{j=1}^{j=r_i} \mathbf{x}_{ij}\mathbf{y}_{ij}^\top$, where \mathbf{x}_{ij} and \mathbf{y}_{ij} are the j -th column vectors of \mathbf{X}_i and \mathbf{Y}_i , and $i \in \{1, 2\}$. Then,

$$\mathbf{W} = \mathbf{X}_1\mathbf{Y}_1^\top \odot \mathbf{X}_2\mathbf{Y}_2^\top = \sum_{j=1}^{j=r_1} \mathbf{x}_{1j}\mathbf{y}_{1j}^\top \odot \sum_{j=1}^{j=r_2} \mathbf{x}_{2j}\mathbf{y}_{2j}^\top = \sum_{k=1}^{k=r_1} \sum_{j=1}^{j=r_2} (\mathbf{x}_{1k}\mathbf{y}_{1k}^\top) \odot (\mathbf{x}_{2j}\mathbf{y}_{2j}^\top). \quad (1)$$

\mathbf{W} is the summation of r_1r_2 number of rank-1 matrices; thus, $\text{rank}(\mathbf{W})$ is bounded above r_1r_2 . \square

Proposition 1 implies that, unlike the low-rank parameterization, a higher-rank matrix can be constructed using the Hadamard product of two inner low-rank matrices, W_1 and W_2 (Refer to Figure 1). If we choose the inner ranks r_1 and r_2 such that $r_1r_2 \geq \min(m, n)$, the constructed matrix can span a full-rank matrix; *i.e.*, FedPara has the minimal parameter property achievable to full-rank.

To apply Proposition 1 to the convolutional layers, we reshape the fourth-order tensor kernel to the matrix as $\mathbb{R}^{O \times I \times K_1 \times K_2} \rightarrow \mathbb{R}^{O \times (IK_1K_2)}$, where O, I, K_1 , and K_2 are the output channels, the input channels, and the kernel sizes, respectively. That is, our parameterization spans convolution filters with a few basis filters of size $I \times K_1 \times K_2$. We can control the number of parameters by changing the inner ranks r_1 and r_2 , respectively, but we have the following useful proposition to set a minimal number of parameters with a maximal rank.

Proposition 2 Given $R \in \mathbb{N}$, $r_1 = r_2 = R$ is the unique optimal choice of the following criteria,

$$\arg \min_{r_1, r_2 \in \mathbb{N}} (r_1 + r_2)(m + n) \quad \text{s.t.} \quad r_1r_2 \geq R^2, \quad (2)$$

and its optimal value is $2R(m+n)$.

Proof. We use arithmetic-geometric mean inequality and the given constraint. We have

$$(r_1 + r_2)(m + n) \geq 2\sqrt{r_1r_2}(m + n) \geq 2R(m + n). \quad (3)$$

The equality holds if and only if $r_1 = r_2 = R$ by the arithmetic-geometric mean inequality. \square

Eq. 2 implies the criteria that minimize the number of weight parameters used in our parameterization with the target rank constraint of the constructed matrix as R^2 . Proposition 2 provides an efficient way to set the hyper-parameters. It implies that, if we set $r_1=r_2=R$ and $R^2 \geq \min(m, n)$, FedPara is highly likely to have no low-rank restriction² even with much fewer parameters than that of a naïve

²Its corollary and empirical evidence can be found in the supplementary material. Under Proposition 2, $R^2 \geq \min(m, n)$ is a necessary and sufficient condition for achieving a maximal rank.

weight, i.e., $2R(m+n) \ll mn$. Moreover, given the same number of parameters, $\text{rank}(\mathbf{W})$ of FedPara is higher than that of the naïve low-rank parameterization by a square factor, as shown in Figure 1. We further extend our parameterization to the tensor structure as follows:

Proposition 3 Let $\mathcal{T}_1, \mathcal{T}_2 \in \mathbb{R}^{R \times R \times k_3 \times k_4}$, $\mathbf{X}_1, \mathbf{X}_2 \in \mathbb{R}^{k_1 \times R}$, $\mathbf{Y}_1, \mathbf{Y}_2 \in \mathbb{R}^{k_2 \times R}$, $R \leq \min(k_1, k_2)$ and the convolution kernel be $\mathcal{W} := (\mathcal{T}_1 \times_1 \mathbf{X}_1 \times_2 \mathbf{Y}_1) \odot (\mathcal{T}_2 \times_1 \mathbf{X}_2 \times_2 \mathbf{Y}_2)$. Then, the rank of the kernel satisfies $\text{rank}(\mathcal{W}^{(1)}) = \text{rank}(\mathcal{W}^{(2)}) \leq R^2$.

Proof. According to Rabanser *et al.* [29], the 1st and 2nd unfolding of tensors can be expressed as

$$\begin{aligned} \mathcal{W}^{(1)} &= (\mathbf{X}_1 \mathcal{T}_1^{(1)} (\mathbf{I}^{(4)} \otimes \mathbf{I}^{(3)} \otimes \mathbf{Y}_1)^\top) \odot (\mathbf{X}_2 \mathcal{T}_2^{(1)} (\mathbf{I}^{(4)} \otimes \mathbf{I}^{(3)} \otimes \mathbf{Y}_2)^\top), \\ \mathcal{W}^{(2)} &= (\mathbf{Y}_1 \mathcal{T}_1^{(2)} (\mathbf{I}^{(4)} \otimes \mathbf{I}^{(3)} \otimes \mathbf{X}_1)^\top) \odot (\mathbf{Y}_2 \mathcal{T}_2^{(2)} (\mathbf{I}^{(4)} \otimes \mathbf{I}^{(3)} \otimes \mathbf{X}_2)^\top), \end{aligned} \quad (4)$$

where $\mathbf{I}^{(3)} \in \mathbb{R}^{k_3 \times k_3}$ and $\mathbf{I}^{(4)} \in \mathbb{R}^{k_4 \times k_4}$ are identity matrices. Since $\mathcal{W}^{(1)}$ and $\mathcal{W}^{(2)}$ are matrices, we apply the same process used in Eq. 1, then we obtain $\text{rank}(\mathcal{W}^{(1)}) = \text{rank}(\mathcal{W}^{(2)}) \leq R^2$. \square

Proposition 3 is the extension of Proposition 1 but can be applied to the convolutional layer without reshaping. If $k_1 = O, k_2 = I, k_3 = K_1$, and $k_4 = K_2$, the number of parameters are $2R(O + IK_1K_2)$ in Proposition 1 and $2R(O + I + RK_1K_2)$ in Proposition 3. When $O = I, R = \sqrt{O}$ and $K_1, K_2 \ll O$, the number of parameters is $\mathcal{O}(ROK_1K_2)$ and $\mathcal{O}(RO)$, respectively. Given $O = 256, I = 256, K_1 = K_2 = 3$ and $R = 16$, both Propositions 1 and 3 can achieve full-rank because $R^2 = 256$. Compared to the original parameterization, Propositions 1 and 3 use 7.2 and 28.1 times fewer parameters, respectively. In this regard, we use Proposition 3 mainly because the tensor method is more effective for common convolutional models.

Optionally, we employ non-linearity and the Jacobian correction regularization, of which details can be found in the supplementary material. These techniques improve the accuracy and convergence stability but not essential. Depending on the resources of devices, these techniques can be omitted.

3.3 pFedPara: A Personalization Application

Data are heterogeneous and personal due to different characteristics of each client, such as usage times and habits. To tackle this personal scenario, FedPer [30] was proposed, where it distinguishes between global and local layers in the model. Clients only transfer global layers and keep local ones on each device. Thus, the global layers are trained collaboratively to extract general features, whereas the local layers are biased to each user.

With FedPara, we propose a personalization application, pFedPara, in which the Hadamard product is a bridge between the global inner weight \mathbf{W}_1 and the local inner weight \mathbf{W}_2 ; the weight \mathbf{W}_1 is transferred to the server while \mathbf{W}_2 is kept in a local device during FL. Since pFedPara transfers a half of the parameters compared to FedPara under the same rank condition, the communication efficiency is increased further. The complete personal model is constructed as $\mathbf{W} = \mathbf{W}_1 \odot (\mathbf{W}_2 + \mathbf{1})$, where $(\mathbf{W}_2 + \mathbf{1})$ induces \mathbf{W}_1 to learn globally shared knowledge implicitly and acts as switching.

Conceptually, we can rewrite $\mathbf{W} = \mathbf{W}_1 \odot \mathbf{W}_2 + \mathbf{W}_1 = \mathbf{W}_{per.} + \mathbf{W}_{glo.}$, where $\mathbf{W}_{per.} = \mathbf{W}_1 \odot \mathbf{W}_2$ and $\mathbf{W}_{glo.} = \mathbf{W}_1$. The construction of the final personalized parameter \mathbf{W} in pFedPara can be viewed as an additive model of the global weight $\mathbf{W}_{glo.}$ and the personalizing residue $\mathbf{W}_{per.}$. Intuitively, FedPer and pFedPara are distinguished by their respective global and local split directions, as illustrated in Figure 2. We summarize our algorithms in the supplementary material.

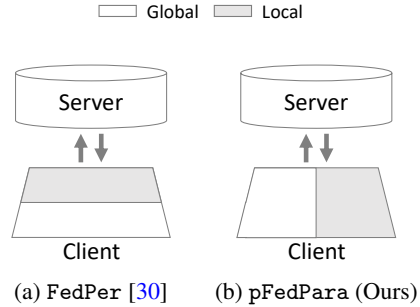


Figure 2: Diagrams of (a) FedPer and (b) pFedPara. The global part is transferred to the server, and the local part remains in each client’s device.

Table 1: Accuracy comparison between VGG16_{low} and VGG16_{FedPara}. We set the target rounds T as 200 for CIFAR-10, 400 for CIFAR-100, and 300 for CINIC-10.

Models	CIFAR-10 ($T = 200$)		CIFAR-100 ($T = 400$)		CINIC-10 ($T = 300$)	
	IID	non-IID	IID	non-IID	IID	non-IID
VGG16 _{low}	77.62	67.75	34.16	30.30	63.98	60.80
VGG16 _{FedPara} (Ours)	82.88	71.35	45.78	43.94	70.35	64.95

4 Experiments

We evaluate our FedPara in terms of communication costs, the number of parameters, and compatibility with other FL methods. We also evaluate pFedPara in three different non-IID scenarios. We use the standard FL algorithm, FedAvg, as a backbone optimizer in all experiments except for the compatibility experiments. We use PyTorch Distributed library [31] and 8 NVIDIA GeForce RTX 3090 GPUs. More details and additional experiments can be found in the supplementary material.

4.1 Setup

Datasets. In FedPara experiments, we use three popular classification datasets: CIFAR-10, CIFAR-100 [32] and CINIC-10 [33]. We split the datasets randomly into 100 partitions for the CIFAR-10 and CINIC-10 IID settings and 50 partitions for the CIFAR-100 IID setting. For non-IID settings, we use the Dirichlet distribution for random partitioning and set the Dirichlet parameter α as 0.5 as suggested by He et al. [34]. We assign one partition to each client and sample 16% of clients for an update at each round during FL. In pFedPara experiments, we use the subset of handwritten datasets: MNIST [35] and FEMNIST [36]. For the non-IID setting with MNIST, we follow McMahan et al. [1], where each of 100 clients has at most two classes.

Models. For FedPara, we mainly use the VGG16 architecture [3], in which we replace the batch normalization with the group normalization as suggested by Hsieh et al. [37]. VGG16_{ori.} stands for the original VGG16, VGG16_{low} the one with the low-rank tensor parameterization in a Tucker form by following TKD [27], and VGG16_{FedPara} the one with our FedPara. For pFedPara, we use two FC layers as suggested by McMahan et al. [1].

Rank Hyper-parameter. We adjust the inner rank of \mathbf{W}_1 and \mathbf{W}_2 as $r = (1-\gamma)r_{min} + \gamma r_{max}$, where r_{min} is the minimum rank allowing FedPara to achieve a full-rank by Proposition 2, r_{max} is the maximum rank such that the number of FedPara’s parameters do not exceed the number of original parameters, and $\gamma \in [0, 1]$. We can independently tune γ for each layer in the model, but we fix the same γ for all layers for simplicity. Note that γ determines the number of parameters.

4.2 Quantitative Results

Capacity. In this experiment, we validate the propositions stating that our FedPara achieves a higher rank than the low-rank parameterization given the same number of parameters. We train VGG16_{low} and VGG16_{FedPara} for the same target rounds, T , and use 10.25% and 10.15% of the VGG16_{ori.} parameters, respectively, to be comparable. As shown in Table 1, VGG16_{FedPara} surpasses VGG16_{low} on all the benchmarks for both IID and non-IID settings with noticeable margins. This experiment shows that the low-rank parameterization has limitations in expressiveness and accuracy degradation, whereas FedPara has higher accuracy, which demonstrates that our FedPara has a larger capacity than the low-rank parameterization. Moreover, in the following experiments, we show FedPara can achieve comparable accuracy with the original counterpart.

Communication Cost. We compare VGG16_{FedPara} and VGG16_{ori.} in terms of accuracy and communication costs. FL methods typically measure the required rounds to achieve the target accuracy as communication costs, but we instead assess total transferred bit sizes, $2 \times (\#participants) \times (\text{model size}) \times (\#rounds)$, which considers up-/down- link and is a more practical communication cost metric. Depending on the difficulty of the datasets, we set the model size to 10.1% for CIFAR-10, 29.4% for CIFAR-100, and 21.8% for CINIC-10 of VGG16_{ori.}.

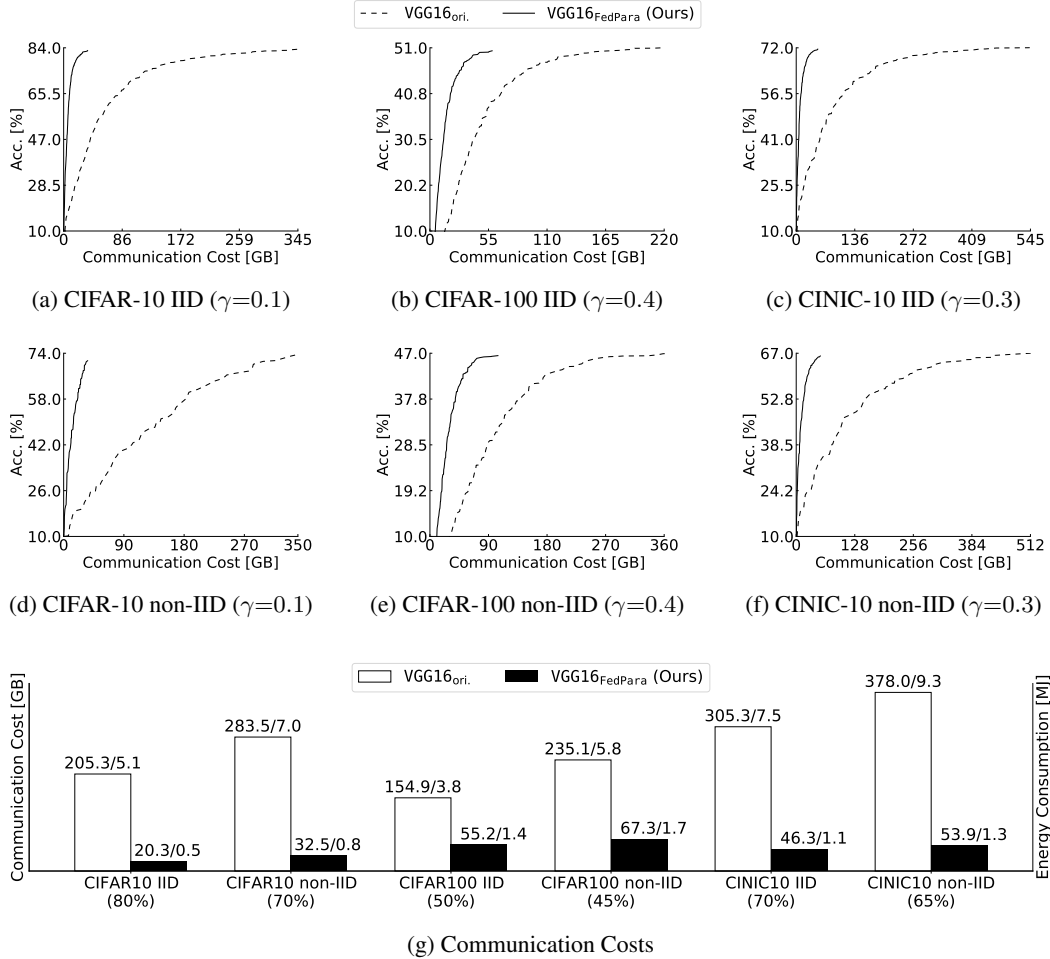


Figure 3: (a-f): Accuracy [%] (y -axis) vs. communication costs [GBytes] (x -axis) of VGG16_{ori.} and VGG16_{FedPara}. Broken line and solid line represent VGG16_{ori.} and VGG16_{FedPara}, respectively. (g): Size comparison of transferred parameters, which can be expressed as communication costs [GBytes] (left y -axis) or energy consumption [MJ] (right y -axis), for the same target accuracy. The white bars are the results of VGG16_{ori.} and the black bars are the results of VGG16_{FedPara}. The target accuracy is denoted in the parentheses under the x -axis of (g).

As shown in Figures 3a-3f, VGG16_{FedPara} has comparable accuracy but requires much lower communication costs than VGG16_{ori.}. Figure 3g shows communication costs and energy consumption required for model training to achieve the target accuracy; we compute the energy consumption by the energy model of user-to-data center topology [6]. VGG16_{FedPara} needs 2.8 to 10.1 times fewer communication costs and energy consumption than VGG16_{ori.} to achieve the same target accuracy.

Model Parameter Ratio. We analyze how the number of parameters controlled by the rank ratio γ affects the accuracy of FedPara. As shown in Figure 4, the VGG16_{FedPara}'s accuracy mostly increases as the number of parameters increases. VGG16_{FedPara} can achieve even higher accuracy than VGG16_{ori.}. It is consistent with the reports from the prior works [38, 39] on model compression, where reduced parameters often lead to accuracy improvement, *i.e.*, regularization effects.

Compatibility. We integrate the FedPara-based model with other FL optimizers to show that our FedPara is compatible with them. We measure the accuracy during the target rounds and the required rounds to achieve the target accuracy. Table 2 shows that VGG16_{FedPara} combined with the current state-of-the-art method, FedDyn, is the best among other combinations. Thereby, we can further save the communication costs by combining FedPara with other efficient FL approaches.

Personalization. We evaluate pFedPara. In this experiment, we assume no sub-sampling of clients for an update. We train two FC layers using four algorithms, Local, FedAvg, FedPer, and

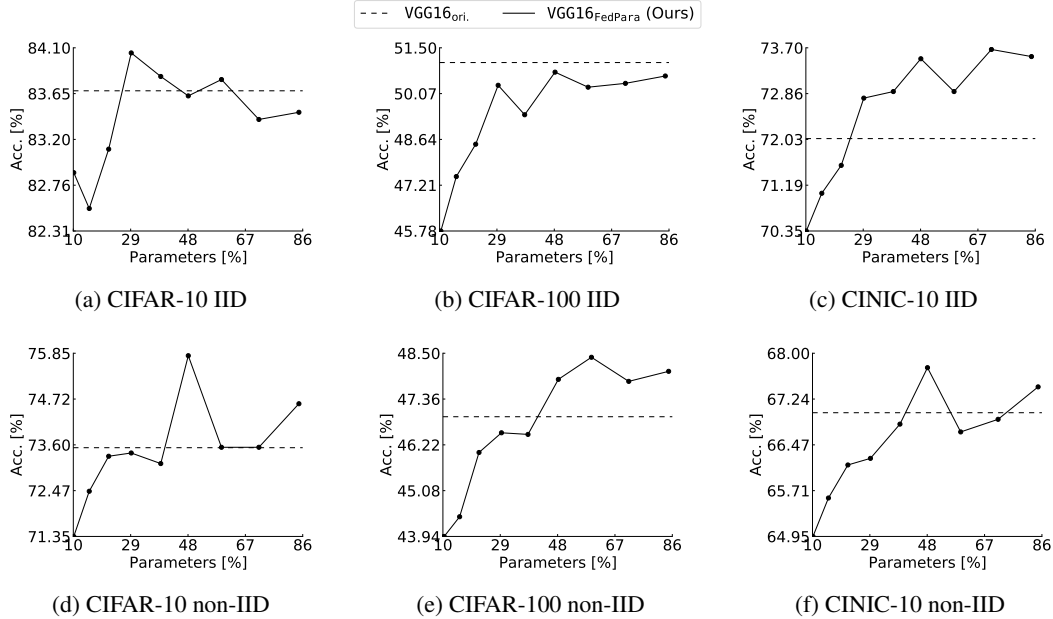


Figure 4: Test accuracy [%] (y -axis) vs. parameters ratio [%] (x -axis) of VGG16_{FedPara} after the target round on various datasets. Broken line represents VGG16_{ori} with no parameter reduction, and solid line VGG16_{FedPara} adjusted by γ from 0.1 to 0.9 in 0.1 increments. The target rounds follow Table 1.

Table 2: The compatibility of FedPara with other learning algorithms. The first row is the accuracy of FedPara combined with other learning algorithms on the CIFAR-10 IID setting after 200 rounds, and the second row is the required rounds to achieve the target accuracy 80%.

	FedAvg [1]	FedProx [7]	SCAFFOLD [8]	FedDyn [9]	FedAdam [11]
Accuracy ($T = 200$)	82.88	78.95	84.72	86.05	82.48
Round (80%)	110	-	92	80	117

pFedPara, with ten clients on respective FEMNIST and MNIST. Local denotes the local models trained only using their own local data; FedAvg the global model trained by the FedAvg optimization; and FedPer and pFedPara the personalized models of which the first layer (FedPer) and the half of inner matrices (pFedPara) are trained by sharing with the server, respectively, while the other parts are locally updated. We validate these algorithms on three scenarios as described in Figure 5.

In Scenario 1 (Figure 5a), the Local accuracy is higher than those of FedAvg and FedPer because each client has sufficient data. Nevertheless, pFedPara surpasses the other methods. In Scenario 2 (Figure 5b), the FedAvg accuracy is higher than that of Local because local data are too scarce to train the local models. The FedPer accuracy is also lower than that of FedAvg because the last layer of FedPer does not exploit other clients' data; thus, FedPer is susceptible to a lack of local data. The higher performance of pFedPara shows that our pFedPara can take advantage of the wealth of distributed data in the personalized setup. In Scenario 3 (Figure 5c), the FedAvg accuracy is much lower than the other methods due to the highly-skewed data distribution. The other methods show comparable accuracy. In most scenarios, pFedPara performs better or favorably against the others. It validates that pFedPara can train the personalized models collaboratively and robustly.

Additionally, both pFedPara and FedPer save the communication costs because they partially transfer parameters; pFedPara transfers 3.4 times fewer parameters, whereas FedPer transfers 1.07 times fewer than the original model in each round. The reduction of FedPer is negligible because it is designed to transfer all the layers except the last one. Contrarily, the reduction of pFedPara is three times larger than FedPer because all the layers of pFedPara are factorized by the Hadamard product during training, and only a half of each layer's parameters are transmitted. Thus pFedPara is far more favorable in terms of both personalization performance and communication efficiency in FL.

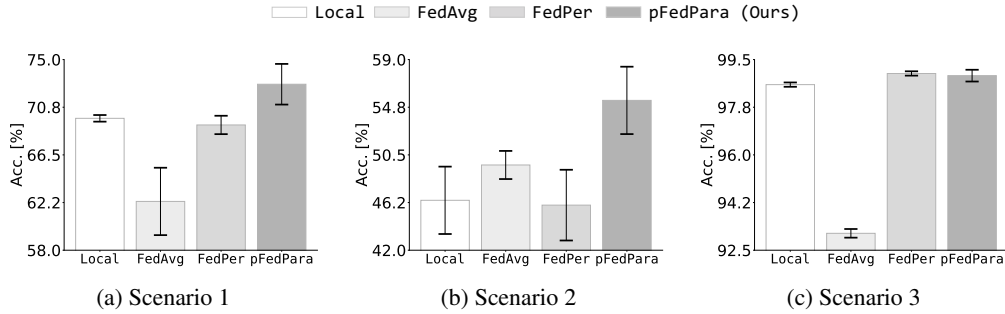


Figure 5: Average test accuracy over ten local models across four algorithms. (a) 100% of local training data on FEMNIST are used with the non-IID setting, which mimics enough local data to train and evaluates each local model on their own data. (b) 20% of local training data on FEMNIST are used with the non-IID setting, which mimics insufficient local data to train local models. (c) 100% of local training data on MNIST are used with the highly-skew non-IID setting, where each client has at most two classes. 95% confidence intervals are presented with five repetitions.

5 Discussion and Conclusion

To overcome the communication bottleneck in FL, we propose a new parameterization method, FedPara, and its personalized version, pFedPara. We demonstrated that both FedPara and pFedPara can significantly reduce communication overheads with minimal performance degradation or better performance over the original counterpart at times. Achieving this trade-off was not possible to the traditional low-rank parameterization because rank constraints limit its expressible range space. In contrast, even with a strong low-rank constraint, FedPara has no such limitation and can achieve a full-rank matrix and tensor by virtue of our proposed low-rank Hadamard product parameterization. These favorable properties enable communication-efficient FL, of which regimes have not been achieved by the previous optimization-based FL approaches. We conclude our work by discussing societal impact, limitations, and future directions. **Limitations.** FedPara conducts multiplications many times, including the Hadamard product, to construct the weights of the layers. These multiplications may potentially be more susceptible to gradient exploding, vanishing, dead neurons, or numerical instability than the low-rank parameterization with an arbitrary initialization. In our experiments, we have not observed such issues with He initialization [40] yet. Nonetheless, we can further investigate an advanced initialization more suitable to our model as future work.

Negative Societal Impact. Although FL is privacy-preserving distributed learning, personal information may be leaked due to the adversary who hijacks the model intentionally during FL. Like other FLs, this risk is also shared with FedPara due to communication. Without care, the private data may be revealed by the membership inference or reconstruction attacks [41]. The local parameters in our pFedPara could be used as a private key to acquire the complete personal model, which would reduce a chance for the full model to be hijacked. It would be interesting to investigate whether our pFedPara guarantees privacy preserving or the way to improve robustness against those risks.

Another concern introduced by FL is limited-service access to the people living in countries having inferior communication infrastructure, which may raise human rights concerns including discrimination, excluding, *etc.* It is due to a larger bandwidth requirement of FL to transmit larger models. Our work may broaden the countries capable of FL by reducing required bandwidths, whereby it may contribute to addressing the technology gap between regions.

Positive Societal Impact. The communication efficiency of our FedPara directly leads to noticeable energy-saving effects in the FL scenario. It can contribute to reducing the battery consumption of IoT devices and fossil fuels used to generate electricity. Moreover, compared to the optimization-based FL approaches that reduce necessary communication rounds, our method allows more clients to participate in each learning round under the fixed bandwidth, which would improve convergence speed and accuracy further.

References

- [1] Brendan McMahan, Eider Moore, Daniel Ramage, Seth Hampson, and Blaise Aguera y Arcas. Communication-efficient learning of deep networks from decentralized data. In *Artificial Intelligence and Statistics (AISTATS)*, 2017.
- [2] SPEEDTEST. <https://www.speedtest.net/global-index>. Accessed: 2021-05-26.
- [3] Karen Simonyan and Andrew Zisserman. Very deep convolutional networks for large-scale image recognition. In *International Conference on Learning Representations (ICLR)*, 2015.
- [4] Kaiming He, Xiangyu Zhang, Shaoqing Ren, and Jian Sun. Deep residual learning for image recognition. In *IEEE Conference on Computer Vision and Pattern Recognition (CVPR)*, 2016.
- [5] Sarika Yadav and Rama Shankar Yadav. A review on energy efficient protocols in wireless sensor networks. *Wireless Networks*, 22(1):335–350, 2016.
- [6] Ming Yan, Chien Aun Chan, André F Gyga, Jinyao Yan, Leith Campbell, Ampalavanapillai Nirmalathas, and Christopher Leckie. Modeling the total energy consumption of mobile network services and applications. *Energies*, 12(1):184, 2019.
- [7] Tian Li, Anit Kumar Sahu, Manzil Zaheer, Maziar Sanjabi, Ameet Talwalkar, and Virginia Smith. Federated optimization in heterogeneous networks. In *Machine Learning and Systems (MLSys)*, 2020.
- [8] Sai Praneeth Karimireddy, Satyen Kale, Mehryar Mohri, Sashank Reddi, Sebastian Stich, and Ananda Theertha Suresh. Scaffold: Stochastic controlled averaging for federated learning. In *International Conference on Machine Learning (ICML)*, 2020.
- [9] Durmus Alp Emre Acar, Yue Zhao, Ramon Matas, Matthew Mattina, Paul Whatmough, and Venkatesh Saligrama. Federated learning based on dynamic regularization. In *International Conference on Learning Representations (ICLR)*, 2021.
- [10] Felix Yu, Ankit Singh Rawat, Aditya Menon, and Sanjiv Kumar. Federated learning with only positive labels. In *International Conference on Machine Learning (ICML)*, 2020.
- [11] Sashank J. Reddi, Zachary Charles, Manzil Zaheer, Zachary Garrett, Keith Rush, Jakub Konečný, Sanjiv Kumar, and Hugh Brendan McMahan. Adaptive federated optimization. In *International Conference on Learning Representations (ICLR)*, 2021.
- [12] Amirhossein Reisizadeh, Aryan Mokhtari, Hamed Hassani, Ali Jadbabaie, and Ramtin Pedarsani. Fedpaq: A communication-efficient federated learning method with periodic averaging and quantization. In *Artificial Intelligence and Statistics (AISTATS)*, 2020.
- [13] Farzin Haddadpour, Mohammad Mahdi Kamani, Aryan Mokhtari, and Mehrdad Mahdavi. Federated learning with compression: Unified analysis and sharp guarantees. In *Artificial Intelligence and Statistics (AISTATS)*, 2021.
- [14] Peter Kairouz, H Brendan McMahan, Brendan Avent, Aurélien Bellet, Mehdi Bennis, Arjun Nitin Bhagoji, Keith Bonawitz, Zachary Charles, Graham Cormode, Rachel Cummings, et al. Advances and open problems in federated learning. *arXiv preprint arXiv:1912.04977*, 2019.
- [15] Hao Yu, Sen Yang, and Shenghuo Zhu. Parallel restarted sgd with faster convergence and less communication: Demystifying why model averaging works for deep learning. In *AAAI Conference on Artificial Intelligence (AAAI)*, 2019.
- [16] Sebastian U. Stich. Local SGD converges fast and communicates little. In *International Conference on Learning Representations (ICLR)*, 2019.
- [17] Xiang Li, Kaixuan Huang, Wenhao Yang, Shusen Wang, and Zhihua Zhang. On the convergence of fedavg on non-iid data. In *International Conference on Learning Representations (ICLR)*, 2020.
- [18] Honglin Yuan and Tengyu Ma. Federated accelerated stochastic gradient descent. In *Advances in Neural Information Processing Systems (NeurIPS)*, 2020.
- [19] Enmao Diao, Jie Ding, and Vahid Tarokh. Hetero{fl}: Computation and communication efficient federated learning for heterogeneous clients. In *International Conference on Learning Representations (ICLR)*, 2021.
- [20] Dan Alistarh, Demjan Grubic, Jerry Li, Ryota Tomioka, and Milan Vojnovic. Qsgd: Communication-efficient sgd via gradient quantization and encoding. In *Advances in Neural Information Processing Systems (NeurIPS)*, 2017.

- [21] Jeremy Bernstein, Yu-Xiang Wang, Kamyar Azizzadenesheli, and Animashree Anandkumar. signSGD: Compressed optimisation for non-convex problems. In *International Conference on Machine Learning (ICML)*, 2018.
- [22] Wei Wen, Cong Xu, Feng Yan, Chunpeng Wu, Yandan Wang, Yiran Chen, and Hai Li. Terngrad: Ternary gradients to reduce communication in distributed deep learning. In *Advances in Neural Information Processing Systems (NeurIPS)*, 2017.
- [23] Dan Alistarh, Torsten Hoefer, Mikael Johansson, Nikola Konstantinov, Sarit Khirirat, and Cedric Renggli. The convergence of sparsified gradient methods. In *Advances in Neural Information Processing Systems (NeurIPS)*, 2018.
- [24] Yujun Lin, Song Han, Huizi Mao, Yu Wang, and Bill Dally. Deep gradient compression: Reducing the communication bandwidth for distributed training. In *International Conference on Learning Representations (ICLR)*, 2018.
- [25] Vadim Lebedev, Yaroslav Ganin, Maksim Rakhuba, Ivan V. Oseledets, and Victor S. Lempitsky. Speeding-up convolutional neural networks using fine-tuned cp-decomposition. In *International Conference on Learning Representations (ICLR)*, 2015.
- [26] Cheng Tai, Tong Xiao, Xiaogang Wang, and Weinan E. Convolutional neural networks with low-rank regularization. In *International Conference on Learning Representations (ICLR)*, 2016.
- [27] Anh-Huy Phan, Konstantin Sobolev, Konstantin Sozykin, Dmitry Ermilov, Julia Gusak, Petr Tichavský, Valeriy Glukhov, Ivan Oseledets, and Andrzej Cichocki. Stable low-rank tensor decomposition for compression of convolutional neural network. In *European Conference on Computer Vision (ECCV)*, 2020.
- [28] Jakub Konečný, H Brendan McMahan, Felix X Yu, Peter Richtárik, Ananda Theertha Suresh, and Dave Bacon. Federated learning: Strategies for improving communication efficiency. *arXiv preprint arXiv:1610.05492*, 2016.
- [29] Stephan Rabanser, Oleksandr Shchur, and Stephan Günnemann. Introduction to tensor decompositions and their applications in machine learning. *arXiv preprint arXiv:1711.10781*, 2017.
- [30] Manoj Ghuhari Arivazhagan, Vinay Aggarwal, Aaditya Kumar Singh, and Sunav Choudhary. Federated learning with personalization layers. *arXiv preprint arXiv:1912.00818*, 2019.
- [31] Adam Paszke, Sam Gross, Francisco Massa, Adam Lerer, James Bradbury, Gregory Chanan, Trevor Killeen, Zeming Lin, Natalia Gimelshein, Luca Antiga, Alban Desmaison, Andreas Kopf, Edward Yang, Zachary DeVito, Martin Raison, Alykhan Tejani, Sasank Chilamkurthy, Benoit Steiner, Lu Fang, Junjie Bai, and Soumith Chintala. Pytorch: An imperative style, high-performance deep learning library. In *Advances in Neural Information Processing Systems (NeurIPS)*, 2019.
- [32] Alex Krizhevsky, Geoffrey Hinton, et al. Learning multiple layers of features from tiny images. Technical report, Citeseer, 2009.
- [33] Luke N Darlow, Elliot J Crowley, Antreas Antoniou, and Amos J Storkey. Cinic-10 is not imagenet or cifar-10. *arXiv preprint arXiv:1810.03505*, 2018.
- [34] Chaoyang He, Songze Li, Jinhyun So, Mi Zhang, Hongyi Wang, Xiaoyang Wang, Praneeth Vepakomma, Abhishek Singh, Hang Qiu, Li Shen, et al. Fedml: A research library and benchmark for federated machine learning. *Advances in Neural Information Processing Systems Workshops (NeurIPSW)*, 2020.
- [35] Yann LeCun, Léon Bottou, Yoshua Bengio, and Patrick Haffner. Gradient-based learning applied to document recognition. *Proceedings of the IEEE*, 86(11):2278–2324, 1998.
- [36] Sebastian Caldas, Sai Meher Karthik Duddu, Peter Wu, Tian Li, Jakub Konečný, H Brendan McMahan, Virginia Smith, and Ameet Talwalkar. Leaf: A benchmark for federated settings. *Advances in Neural Information Processing Systems Workshops (NeurIPSW)*, 2018.
- [37] Kevin Hsieh, Amar Phanishayee, Onur Mutlu, and Phillip Gibbons. The non-iid data quagmire of decentralized machine learning. In *International Conference on Machine Learning (ICML)*, 2020.
- [38] Jian-Hao Luo, Jianxin Wu, and Weiyao Lin. Thinet: A filter level pruning method for deep neural network compression. In *IEEE International Conference on Computer Vision (ICCV)*, 2017.
- [39] Hyeji Kim, Muhammad Umar Karim Khan, and Chong-Min Kyung. Efficient neural network compression. In *IEEE Conference on Computer Vision and Pattern Recognition (CVPR)*, 2019.

- [40] Kaiming He, Xiangyu Zhang, Shaoqing Ren, and Jian Sun. Delving deep into rectifiers: Surpassing human-level performance on imagenet classification. In *IEEE International Conference on Computer Vision (ICCV)*, 2015.
- [41] Maria Rigaki and Sebastian Garcia. A survey of privacy attacks in machine learning. *arXiv preprint arXiv:2007.07646*, 2020.
- [42] Chaoyang He, Murali Annavaram, and Salman Avestimehr. Group knowledge transfer: Federated learning of large cnns at the edge. In *Advances in Neural Information Processing Systems (NeurIPS)*, 2020.
- [43] Diederik P. Kingma and Jimmy Ba. Adam: A method for stochastic optimization. In *International Conference on Learning Representations (ICLR)*, 2015.

Supplementary

In this supplementary material, we present additional details, results, and experiments that are not included in the main paper due to the space limit. The contents of this supplementary material are listed as follows:

A Maximal Rank Property

In this section, we present an additional analysis of our method’s algorithmic behavior in terms of the rank property. With a condition, $R^2 \geq \min(m, n)$, our parameter setting scheme presented in Proposition 2, *i.e.*, $r_1 = r_2$, provides a stronger guarantee as shown in the following corollary to Proposition 2.

Corollary 1 *Under Proposition 2, $R^2 \geq \min(m, n)$ is a necessary and sufficient condition for achieving the maximal rank of $\mathbf{W} = (\mathbf{X}_1 \mathbf{Y}_1^\top) \odot (\mathbf{X}_2 \mathbf{Y}_2^\top) \in \mathbb{R}^{m \times n}$, where $\mathbf{X}_1 \in \mathbb{R}^{m \times r_1}$, $\mathbf{X}_2 \in \mathbb{R}^{m \times r_2}$, $\mathbf{Y}_1 \in \mathbb{R}^{n \times r_1}$, $\mathbf{Y}_2 \in \mathbb{R}^{n \times r_2}$, and $r_1, r_2 \leq \min(m, n)$.*

Proof. We first prove the sufficient condition. Given $r_1 = r_2 = R$ under Proposition 2 and $R^2 \geq \min(m, n)$, $\text{rank}(\mathbf{W}) \leq \min(r_1 r_2, m, n) = \min(R^2, m, n) = \min(m, n)$. The matrix \mathbf{W} has no low-rank restriction; thus the condition, $R^2 \geq \min(m, n)$, is the sufficient condition.

The necessary condition is proved by contraposition; if $R^2 < \min(m, n)$, the matrix \mathbf{W} cannot achieve the maximal rank. Since $r_1 = r_2 = R$ under Proposition 2 and $R^2 < \min(m, n)$, then $\text{rank}(\mathbf{W}) \leq \min(r_1 r_2, m, n) = \min(R^2, m, n) = R^2 < \min(m, n)$. That is, $\text{rank}(\mathbf{W})$ is upper-bounded by R^2 , which is lower than the maximal achievable rank of \mathbf{W} . Therefore, the condition, $R^2 \geq \min(m, n)$, is the necessary condition because the contrapositive is true. \square

Corollary 1 implies that, with $R^2 \geq \min(m, n)$, the constructed weight \mathbf{W} does not have the low-rank limitation, and allows us to define the minimum inner rank as $r_{\min} := \min(\lceil \sqrt{m} \rceil, \lceil \sqrt{n} \rceil)$. If we set $r_1 = r_2 = r_{\min}$, $\text{rank}(\mathbf{W})$ of our FedPara can achieve the maximal rank because $r_1 r_2 = r_{\min}^2 \geq \min(m, n)$ while minimizing the number of parameters.

Empirical test. To demonstrate our propositions empirically, we sample the parameters randomly and count $\text{rank}(\mathbf{W})$. When applying our parameterization to $\mathbf{W} \in \mathbb{R}^{100 \times 100}$, we set $r_{\min} = 10$ by Corollary 1 to Proposition 2. We sample the entries of $\mathbf{X}_1, \mathbf{X}_2, \mathbf{Y}_1, \mathbf{Y}_2 \in \mathbb{R}^{100 \times 10}$ from the standard Gaussian distribution and repeat this experiment 1,000 times.

As shown in Figure 6, we observe that our parameterization achieves the full rank with the probability of 100% but requires 2.5 times fewer entries than the original 100×100 matrix. This empirical result demonstrates that our parameterization can span the full-rank matrix with fewer parameters efficiently.

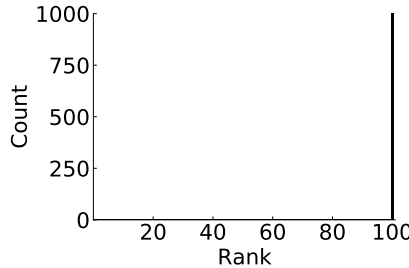


Figure 6: Histogram of $\text{rank}(\mathbf{W})$. We apply FedPara to $\mathbf{W} \in \mathbb{R}^{100 \times 100}$ and set $r_1 = r_2 = 10$. We repeat this experiment 1,000 times.

B Additional Techniques

We devise additional techniques to improve the accuracy and stability of our parameterization. We consider injecting a non-linearity in FedPara and Jacobian correction regularization to further squeeze out the performance and stability. However, as will be discussed later, these are optional.

The first is to apply a non-linear function before the Hadamard product. FedPara composites the weight as $\mathbf{W} = \mathbf{W}_1 \odot \mathbf{W}_2$, and we inject non-linearity as $\mathbf{W} = \sigma(\mathbf{W}_1) \odot \sigma(\mathbf{W}_2)$ as a practical design. This makes our algorithm departing from directly applying the proofs, *i.e.*, empirical heuristics. However, the

Table 3: Accuracy of FedPara with additional techniques. 95% confidence intervals are presented with eight repetitions.

Models	Accuracy
FedPara (base)	82.45 \pm 0.35
+ Tanh	82.42 \pm 0.33
+ Regularization	82.38 \pm 0.30
+ Both	82.52 \pm 0.26

favorable performance of our FedPara regardless of this non-linearity injection in practice suggests that our re-parameterization is a reasonable model to deploy.

The non-linear function $\sigma(\cdot)$ can be any non-linear function such as ReLU, Tanh, and Sigmoid, but ReLU and Sigmoid restrict the range to only positive, whereas Tanh has both negative and positive values of range $[-1, 1]$. The filters may learn to extract the distinct features, such as edge, color, and blob, which require both negative and positive values of the filters. Furthermore, the reasonably bounded range can prevent overshooting a large value by multiplication. Therefore, Tanh is suitable, and we use Tanh through experiments except for those of pFedPara.

The second is the Jacobian correction regularization, which induces that the Jacobians of $\mathbf{X}_1, \mathbf{X}_2, \mathbf{Y}_1,$ and \mathbf{Y}_2 follow the Jacobian of the constructed matrix \mathbf{W} . Suppose that $\mathbf{X}_1, \mathbf{X}_2 \in \mathbb{R}^{m \times r}$ and $\mathbf{Y}_1, \mathbf{Y}_2 \in \mathbb{R}^{n \times r}$ are given. We construct the weight as $\mathbf{W} = \mathbf{W}_1 \odot \mathbf{W}_2$, where $\mathbf{W}_1 = \mathbf{X}_1 \mathbf{Y}_1^\top$ and $\mathbf{W}_2 = \mathbf{X}_2 \mathbf{Y}_2^\top$. Additionally, suppose that the Jacobian of \mathbf{W} with respect to the objective function is given: $\mathbf{J}_\mathbf{W} = \frac{\partial \mathbf{L}}{\partial \mathbf{W}}$. We can compute the Jacobians of $\mathbf{X}_1, \mathbf{X}_2, \mathbf{Y}_1,$ and \mathbf{Y}_2 with respect to the objective function and apply one-step optimization with SGD. For simplicity, we set the momentum and the weight decay to be zero. Then, we can compute the Jacobian of other variables using the chain rule:

$$\begin{aligned} \mathbf{J}_{\mathbf{W}_1} &= \frac{\partial \mathbf{L}}{\partial \mathbf{W}_1} = \mathbf{J}_\mathbf{W} \odot \mathbf{W}_2, & \mathbf{J}_{\mathbf{X}_1} &= \frac{\partial \mathbf{L}}{\partial \mathbf{X}_1} = \mathbf{J}_{\mathbf{W}_1} \mathbf{Y}_1^\top, & \mathbf{J}_{\mathbf{Y}_1} &= \frac{\partial \mathbf{L}}{\partial \mathbf{Y}_1} = \mathbf{X}_1^\top \mathbf{J}_{\mathbf{W}_1}, \\ \mathbf{J}_{\mathbf{W}_2} &= \frac{\partial \mathbf{L}}{\partial \mathbf{W}_2} = \mathbf{J}_\mathbf{W} \odot \mathbf{W}_1, & \mathbf{J}_{\mathbf{X}_2} &= \frac{\partial \mathbf{L}}{\partial \mathbf{X}_2} = \mathbf{J}_{\mathbf{W}_2} \mathbf{Y}_2^\top, & \mathbf{J}_{\mathbf{Y}_2} &= \frac{\partial \mathbf{L}}{\partial \mathbf{Y}_2} = \mathbf{X}_2^\top \mathbf{J}_{\mathbf{W}_2}. \end{aligned} \quad (5)$$

We update the parameters using SGD with the step size η as follows:

$$\begin{aligned} \mathbf{X}'_1 &= \mathbf{X}_1 - \eta \mathbf{J}_{\mathbf{X}_1}, & \mathbf{Y}'_1 &= \mathbf{Y}_1 - \eta \mathbf{J}_{\mathbf{Y}_1}, \\ \mathbf{X}'_2 &= \mathbf{X}_2 - \eta \mathbf{J}_{\mathbf{X}_2}, & \mathbf{Y}'_2 &= \mathbf{Y}_2 - \eta \mathbf{J}_{\mathbf{Y}_2}. \end{aligned} \quad (6)$$

We can compute \mathbf{W}' , which is the constructed weight after one-step optimization:

$$\begin{aligned} \mathbf{W}' &= (\mathbf{X}'_1 \mathbf{Y}'_1{}^\top) \odot (\mathbf{X}'_2 \mathbf{Y}'_2{}^\top) \\ &= \{(\mathbf{X}_1 - \eta \mathbf{J}_{\mathbf{X}_1})(\mathbf{Y}_1^\top - \eta \mathbf{J}_{\mathbf{Y}_1}^\top)\} \odot \{(\mathbf{X}_2 - \eta \mathbf{J}_{\mathbf{X}_2})(\mathbf{Y}_2^\top - \eta \mathbf{J}_{\mathbf{Y}_2}^\top)\} \\ &= \{\mathbf{X}_1 \mathbf{Y}_1^\top - \eta(\mathbf{J}_{\mathbf{X}_1} \mathbf{Y}_1^\top + \mathbf{X}_1 \mathbf{J}_{\mathbf{Y}_1}^\top) + \eta^2 \mathbf{J}_{\mathbf{X}_1} \mathbf{J}_{\mathbf{Y}_1}^\top\} \odot \{\mathbf{X}_2 \mathbf{Y}_2^\top - \eta(\mathbf{J}_{\mathbf{X}_2} \mathbf{Y}_2^\top + \mathbf{X}_2 \mathbf{J}_{\mathbf{Y}_2}^\top) + \eta^2 \mathbf{J}_{\mathbf{X}_2} \mathbf{J}_{\mathbf{Y}_2}^\top\} \\ &= (\mathbf{X}_1 \mathbf{Y}_1^\top) \odot (\mathbf{X}_2 \mathbf{Y}_2^\top) + \eta^4 (\mathbf{J}_{\mathbf{X}_1} \mathbf{J}_{\mathbf{Y}_1}^\top) \odot (\mathbf{J}_{\mathbf{X}_2} \mathbf{J}_{\mathbf{Y}_2}^\top) \\ &\quad - \eta^3 \{(\mathbf{J}_{\mathbf{X}_1} \mathbf{Y}_1^\top + \mathbf{X}_1 \mathbf{J}_{\mathbf{Y}_1}^\top) \odot (\mathbf{J}_{\mathbf{X}_2} \mathbf{J}_{\mathbf{Y}_2}^\top) + (\mathbf{J}_{\mathbf{X}_2} \mathbf{Y}_2^\top + \mathbf{X}_2 \mathbf{J}_{\mathbf{Y}_2}^\top) \odot (\mathbf{J}_{\mathbf{X}_1} \mathbf{J}_{\mathbf{Y}_1}^\top)\} \\ &\quad + \eta^2 \{(\mathbf{J}_{\mathbf{X}_1} \mathbf{Y}_1^\top + \mathbf{X}_1 \mathbf{J}_{\mathbf{Y}_1}^\top) \odot (\mathbf{J}_{\mathbf{X}_2} \mathbf{Y}_2^\top + \mathbf{X}_2 \mathbf{J}_{\mathbf{Y}_2}^\top) + (\mathbf{J}_{\mathbf{X}_2} \mathbf{J}_{\mathbf{Y}_2}^\top) \odot (\mathbf{X}_2 \mathbf{Y}_2^\top) + (\mathbf{J}_{\mathbf{X}_2} \mathbf{J}_{\mathbf{Y}_2}^\top) \odot (\mathbf{X}_1 \mathbf{Y}_1^\top)\} \\ &\quad - \eta \{(\mathbf{J}_{\mathbf{X}_1} \mathbf{Y}_1^\top + \mathbf{X}_1 \mathbf{J}_{\mathbf{Y}_1}^\top) \odot (\mathbf{X}_2 \mathbf{Y}_2^\top) + (\mathbf{J}_{\mathbf{X}_2} \mathbf{Y}_2^\top + \mathbf{X}_2 \mathbf{J}_{\mathbf{Y}_2}^\top) \odot (\mathbf{X}_1 \mathbf{Y}_1^\top)\}. \end{aligned} \quad (7)$$

This shows that gradient descent and ascent are mixed, as shown in the signs of each term. We propose the Jacobian correction regularization to minimize the difference between \mathbf{W}' and $\mathbf{W} - \eta \mathbf{J}_\mathbf{W}$, which induces our parameterization to follow the direction of $\mathbf{W} - \eta \mathbf{J}_\mathbf{W}$. The total objective function consists of the target loss function and the Jacobian correction regularization as:

$$\mathfrak{R} = L(\mathbf{X}_1, \mathbf{X}_2, \mathbf{Y}_1, \mathbf{Y}_2) + \frac{\lambda}{2} \|\mathbf{W}' - (\mathbf{W} - \eta \mathbf{J}_\mathbf{W})\|_2. \quad (8)$$

We evaluate the effects of each technique in Table 3. We train VGG16 with group normalization on the CIFAR-10 IID setting during the same target rounds. We set $\gamma = 0.1$ and $\lambda = 10$. As shown, the model with both Tanh and regularization has higher accuracy and lower variation than the base model. There is a gain in accuracy and variance with both techniques, whereas there is a gain only in variance with only one technique.

Again, note that these additional techniques are not essential for FedPara to work; therefore, we can optionally use these depending on the situation where the device has enough computing power.

C Details of Experiment Setup

In this section, we explain the details of the experiments, including datasets, models, and hyper-parameters.

C.1 Datasets

CIFAR-10. CIFAR-10 [32] is the popular classification benchmark dataset, and the license is MIT license. CIFAR-10 consists of 32×32 resolution images in 10 classes, with 6,000 images per class. We use 50,000 images for training and 10,000 images for testing. For federated learning, we split training images into 100 partitions and assign one partition to each client. For the IID setting, we split the dataset into 100 partitions randomly. For the non-IID setting, we use the Dirichlet distribution and set the Dirichlet parameter as 0.5 as suggested by He et al. [34, 42].

CIFAR-100. CIFAR-100 [32] is the popular classification benchmark dataset, and the license is MIT license. CIFAR-100 consists of 32×32 resolution images in 100 classes, with 6,000 images per class. We use 50,000 images for training and 10,000 images for testing. For federated learning, we split training images into 50 partitions. For the IID setting, we split the dataset into 50 partitions randomly. For the non-IID setting, we use the Dirichlet distribution and set the Dirichlet parameter as 0.5 as suggested by He et al. [34, 42].

CINIC-10. CINIC-10 [33] is a drop-in replacement for CIFAR-10 and also the popular classification benchmark dataset, and the license is MIT license. CINIC-10 consists of 32×32 resolution images in 10 classes and three subsets: training, validation, and test. Each subset has 90,000 images with 9,000 per class, and we do not use the validation subset for training. For federated learning, we split training images into 100 partitions. For the IID setting, we split the dataset into 100 partitions randomly. For the non-IID setting, we use the Dirichlet distribution and set the Dirichlet parameter as 0.5 as suggested by He et al. [34, 42].

MNIST. MNIST [35] is a popular handwritten number image dataset and is made available under the terms of the Creative Commons Attribution-Share Alike 3.0 license. MNIST consists of 70,000 number of 28×28 resolution images in 10 classes. We use 60,000 images are for training and 10,000 images for testing. We do not use MNIST IID-setting, and we split the dataset so that clients have at most two classes as suggested by McMahan et al. [1] for a highly-skew non-IID setting.

FEMNIST. FEMNIST [36] is a handwritten image dataset for federated settings, and the license is BSD-2-Clause license. FEMNIST has 62 classes and 3,550 clients, and each client has 226.83 data samples on average of 28×28 resolution images. FEMNIST is the non-IID dataset labeled by writers.

C.2 Models

VGG16. PyTorch library [31] provides VGG16 with batch normalization, but we replace the batch normalization layers with the group normalization layers as suggested by Hsieh et al. [37] for federated learning. We also modify the FC layers to comply with the number of classes. The dimensions of the output features in the last three FC layers are $512-512-(\#classes)$, sequentially. We do not apply our parameterization to the last three FC layers and set the same γ to all convolutional layers in the model for simplicity.

Two FC layers. In personalization experiments, we use two FC layers as suggested by McMahan et al. [1] but modify the size of the hidden features corresponding to the number of classes in the datasets. The dimensions of the output features in two FC layers are 256 and the number of classes, respectively; *i.e.*, $256-(\#classes)$. We do not use other layers, such as normalization and dropout, and set $\gamma = 0.5$ for pFedPara.

C.3 FedPara & pFedPara

Algorithm 1: FedPara

Input: rounds T , parameters $\mathbf{X}_1, \mathbf{X}_2, \mathbf{Y}_1, \mathbf{Y}_2$

```

for  $t = 1, 2, \dots, T$  do
  Sample the subset  $S$  of clients;
  Transmit  $\mathbf{X}_1, \mathbf{X}_2, \mathbf{Y}_1, \mathbf{Y}_2$  to clients;
  for  $c \in S$  do
     $\mathbf{W} = (\mathbf{X}_1 \mathbf{Y}_1^\top) \odot (\mathbf{X}_2 \mathbf{Y}_2^\top)$ ;
    Optimizer( $\mathbf{W}$ );
    Upload  $\mathbf{X}_1, \mathbf{X}_2, \mathbf{Y}_1, \mathbf{Y}_2$ ;
  end
  Aggregate  $\mathbf{X}_1, \mathbf{X}_2, \mathbf{Y}_1, \mathbf{Y}_2$ ;
end

```

Algorithm 2: pFedPara

Input: rounds T , parameters $\mathbf{X}_1, \mathbf{X}_2, \mathbf{Y}_1, \mathbf{Y}_2$

```

Transmit  $\mathbf{X}_2, \mathbf{Y}_2$  to clients;
for  $t = 1, 2, \dots, T$  do
  Sample the subset  $S$  of clients;
  Transmit  $\mathbf{X}_1, \mathbf{Y}_1$  to clients;
  for  $c \in S$  do
     $\mathbf{W} = (\mathbf{X}_1 \mathbf{Y}_1^\top) \odot (\mathbf{X}_2 \mathbf{Y}_2^\top + \mathbf{1})$ ;
    Optimizer( $\mathbf{W}$ );
    Upload  $\mathbf{X}_1, \mathbf{Y}_1$ ;
  end
  Aggregate  $\mathbf{X}_1, \mathbf{Y}_1$ ;
end

```

We summarize our two methods, FedPara and pFedPara, into Algorithms 1 and 2 for apparent comparison. In these algorithms, we can choose a state-of-the-art optimizer and an aggregate method, but mainly use the

popular and standard algorithm, FedAvg, as a backbone optimizer. As mentioned in Section B, we can consider the additional techniques. In the FedPara experiments, we use the non-linearity function and the regularization to Algorithm 1, and set the regularization coefficient λ as 1.0. In pFedPara experiments, we do not apply the additional techniques to Algorithm 2.

C.4 Hyper-parameters of Backbone Optimizer

FedAvg [1] is the most popular algorithm in federated learning. The server samples S number of clients as a subset in each round, each client of the subset trains the model locally by E number of SGD epochs, and the server aggregates the locally updated models and repeats these processes during the total rounds T . We use FedAvg as a backbone optimization algorithm, and its hyper-parameters of our experiments, such as the initial learning rate η , local batch size B , and learning rate decay τ , are described in Table 4.

Table 4: Hyper-parameters of our FedPara with FedAvg

Models	CIFAR-10		CIFAR-100		CINIC-10		FEMNIST, MNIST
	IID	non-IID	IID	non-IID	IID	non-IID	
K	16	16	8	8	16	16	10
T	200	200	400	400	300	300	100
E	10	5	10	5	10	5	5
B	64	64	64	64	64	64	10
η	0.1	0.1	0.1	0.1	0.1	0.1	0.1-0.01
τ	0.992	0.992	0.992	0.992	0.992	0.992	0.999
λ	1	1	1	1	1	1	0

C.5 Hyper-parameters of Other Optimizers

For compatibility experiment, we combine FedPara with other optimization-based FL algorithms: FedProx [7], SCAFFOLD [8], FedDyn [9], and FedAdam [11]. FedProx [7] imposes a proximal term to the objective function to mitigate heterogeneity; SCAFFOLD [8] allows clients to reduce the variance of gradients by introducing auxiliary variables; FedDyn [9] introduces dynamic regularization to reduce the inconsistency between minima of the local device level empirical losses and the global one; FedAdam employs Adam [43] at the server-side instead of the simple model average.

They need a local optimizer to update the model in each client, and we use the SGD optimizer for a fair comparison, and the SGD configuration is the same as that of FedAvg. The four algorithms have additional hyper-parameters. FedProx has a proximal coefficient μ , and we set μ as 0.1. SCAFFOLD has Option I and Option II to update the control variate, and we use Option II with global learning rate η_g ($= 1.0$). FedDyn has the hyper-parameter α ($= 0.1$) in the regularization. FedAdam uses Adam optimizer to aggregate the updated models at the server-side, and we use the parameters $\beta_1 = 0.9$, $\beta_2 = 0.99$, the global learning rate $\eta_g = 0.01$, and the local learning rate $\eta = 10^{-1.5}$ for Adam optimizer.

D Additional Experiments

In this section, we present additional experiment results, including the convergence speed test according to the communication cost and different rank ratio γ 's, and ResNet18 experiments.

As shown in Figure 7, we compare VGG16_{ori.} and VGG16_{FedPara} with three different γ values. Note that a higher γ uses more parameters than a lower γ . Compared to VGG16_{ori.}, VGG16_{FedPara} achieves comparable accuracy, and even higher accuracy with a high γ . VGG16_{FedPara} also requires fewer communication costs than VGG16_{ori.}.

We demonstrate the consistent effectiveness of our method with another architecture, ResNet18. We also train ResNet18 without replacing batch normalization layers. ResNet18_{ori.} stands for the original ResNet18, ResNet18_{FedPara} the one with our FedPara. We set γ of the first layer, the second layer, and the 1×1 convolution layers as 1.0 and adjust γ of remaining layers to control the ResNet18_{FedPara} size; we set $\gamma = 0.1$ for small model size, $\gamma = 0.6$ for mid model size, and $\gamma = 0.9$ for large model size. To train the models in FL, we set the batch size to 10.

As revealed in Figure 8a, ResNet18_{FedPara} has comparable accuracy and uses fewer communication costs than ResNet18_{ori.}, of which the results are consistent with the VGG16 experiments. Figure 8b shows the communication costs required for model training to achieve the same target accuracy. Our ResNet18_{FedPara}

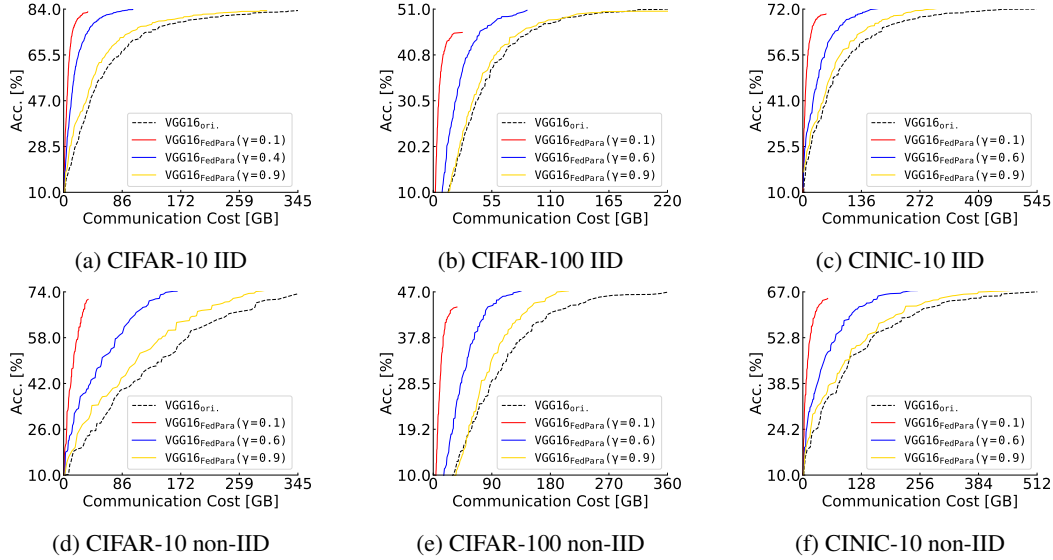


Figure 7: (a-f) Accuracy [%] (y -axis) vs. communication costs [GBytes] (x -axis) of $VGG16_{ori.}$ and $VGG16_{FedPara.}$. Broken black line represents $VGG16_{ori.}$, red solid line $VGG16_{FedPara.}$ with low γ , blue solid line $VGG16_{FedPara.}$ with mid γ , and yellow solid line $VGG16_{FedPara.}$ with high γ

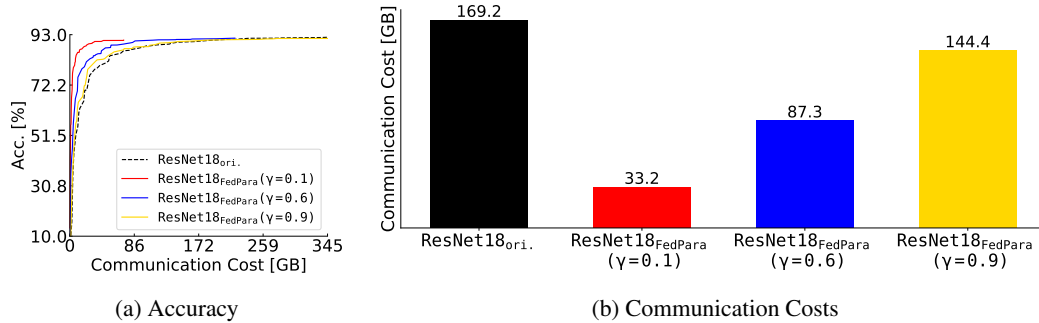


Figure 8: (a) Accuracy [%] (y -axis) vs. communication costs [GBytes] (x -axis) of $ResNet18_{ori.}$ and $ResNet18_{FedPara.}$ with three γ values. (b) Size comparison of transferred parameters, which is expressed as communication costs [GBytes] (y -axis), for the same target accuracy 90%. (a, b): Black represents $ResNet18_{ori.}$, and red, blue, and yellow represents $ResNet18_{FedPara.}$ with low, mid, and high γ , respectively.

needs 1.17 to 5.1 times fewer communication costs than $ResNet18_{ori.}$, and the results demonstrate that FedPara can also be applicable to the ResNet structure.